

Removing chromatic aberration by digital image processing

Soon-Wook Chung

Byoung-Kwang Kim

Woo-Jin Song

Pohang University of Science and Technology
Division of Electrical and Computer Engineering
San 31 Hyoja-Dong, Pohang
Kyungbuk, Korea 790-784
E-mail: WJSong@POSTECH.AC.KR

Abstract. Chromatic aberration is a form of aberration in color optical devices that produces undesirable color fringes along borders within images. It is becoming a more critical problem these days as digital cameras are getting smaller, while the number of picture elements is increasing. We propose a novel method for detecting and eliminating chromatic aberration using image processing. We first analyze the color behavior on edges that do not show chromatic aberration and propose a range limitation for color difference signals. When pixels violate the preceding condition, they can be considered as color fringes caused by chromatic aberration. Corrected pixel values are generated to eliminate the chromatic aberrations. The proposed algorithm corrects both lateral and longitudinal aberration in an image, and experimental results are provided to demonstrate its efficacy. © 2010 Society of Photo-Optical Instrumentation Engineers. [DOI: 10.1117/1.3455506]

Subject terms: chromatic aberration; color fringe; digital camera; image enhancement.

Paper 090751R received Sep. 26, 2009; revised manuscript received Mar. 23, 2010; accepted for publication Apr. 14, 2010; published online Jun. 23, 2010.

1 Introduction

Every optical system that uses lenses suffers from aberrations that occur due to the refractive characteristics of the lenses.¹ Chromatic aberration is one type of aberration in color optical devices. It is well known that visible light is made of a spectrum of colors and when these colors go through a lens, they all have their unique indices of refraction. Thus, the colors bend at slightly different angles as they reach the image plane. There are two forms of chromatic aberration:² lateral aberration and longitudinal aberration. In lateral aberration, all the color components are well focused on the image plane, but displacement or geometric shift between each color component occurs. In longitudinal aberration, the different foci for each color component cause color blurs in the acquired image. Figure 1(a) shows an image acquired with a digital single lens reflex (DSLR) camera that has been degraded with both types of aberration simultaneously. In Fig. 1(b), an enlarged image of the top one-third of Fig. 1(a), we can easily identify the thin red color fringes in the bottom part of the area marked A. And above these red fringes, thick blue fringes are also visible. Observing the RGB intensity along the vertical dotted line in Fig. 1(b) [see Fig. 1(c)], the thin red color fringes are produced because the red signal has been geometrically shifted for about 2 pixels due to lateral aberration. In contrast, the thick blue fringes for about 8 pixels of width are created because the blue signal in this edge has been blurred due to longitudinal aberration. From this example, although the effects of each aberration are very different, it can be determined that both aberrations produce similar color fringes along the edges of an image in either case.^{3,4} Chromatic aberration is becoming a more serious

problem these days as digital cameras are getting smaller, while the number of picture elements is increasing.⁵

Optimal lens design techniques^{6–11} have been proposed to reduce chromatic aberration. These approaches alleviate chromatic aberration by using multiple lenses with different optical indices, e.g., the achromatic doublet,¹² or by improving the lens characteristics.⁹ These corrections, however, have been effective only for the zones near the optical axis, and these hardware solutions can be used only in large cameras and increase their cost.

Because of the high cost of the lens design solutions, active lens control systems^{13,14} have been studied to deal with chromatic aberration. The purpose of the active lens control is to get the best focused image for each color component by slightly shifting the image plane forward and backward for each color. This solution requires *a priori* knowledge about the magnification factor and the image plane shift degree.¹³

As alternatives to these hardware approaches, algorithms using image processing have been suggested.^{4,15–18} These image processing algorithms concentrate on reducing only the lateral aberration, so the effects of the longitudinal aberration remain. They also need to estimate the center point of the aberration for accurate correction while assuming that the aberration center is only the center of the acquired image. The aberration center is often different from the image center due to the complexity of multilens systems.¹⁹ Most of these methods require *a priori* information, such as the precalibrated test pattern information or the camera setting information like the focal length at the time the image was acquired.

Recently, an algorithm correcting chromatic aberration using only a single degraded image²⁰ has been suggested. This method first models the whole process of the imaging

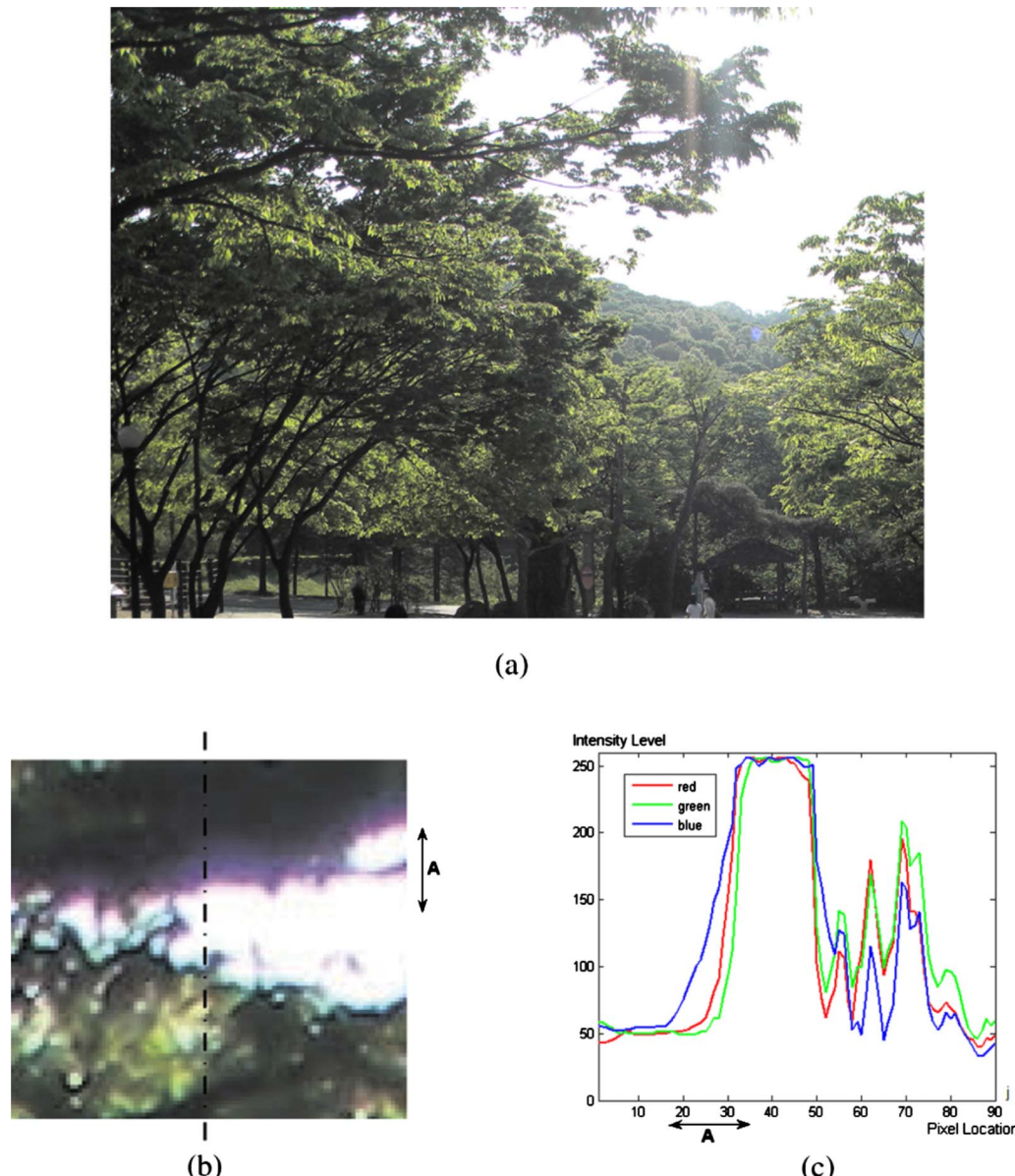


Fig. 1 Degraded image acquired with a DSLR camera. (a) Image of size 1536×2048 pixels. (b) Enlarged image of the top one-third of (a) (approximately 10-pixel width of color fringes are found in the area marked A). (c) RGB intensity along vertical dotted line of (b). (Color online only.)

pipeline and then estimates every simplified step of the pipeline to correct both the lateral and longitudinal aberration.

Other algorithms for measurement and elimination of chromatic aberration in microscope implementation have been proposed.^{21–24} However, these techniques are not applicable to the ordinary camera imaging system.

In spite of the many effective methods available, faster and simpler algorithms are still necessary for many applications such as low-cost digital web cameras or cellular phones with built-in cameras. In this paper, we propose an image processing method that removes color fringes, regardless of whether they were caused by lateral or longitudinal aberration, for a single degraded image. This method exploits an observation that the color intensity of the red

and blue signals are degraded due to the fact that cameras are typically focused on the green signal. We first analyze the color behavior related to the color difference signals on edges that do not show chromatic aberration and propose a condition for the color difference signals on those edges. When the pixels violate the preceding condition, they can be considered as color fringes caused by chromatic aberration. Then, an output pixel value is calculated to eliminate the color fringes. Because the algorithm requires no *a priori* knowledge, it can be easily applied to any image.

This paper is organized as follows. In Sec. 2, we suggest a range limitation condition for the color difference signals on edges by analyzing the color behavior on normal edges without chromatic aberration. In Sec. 3, the details of our

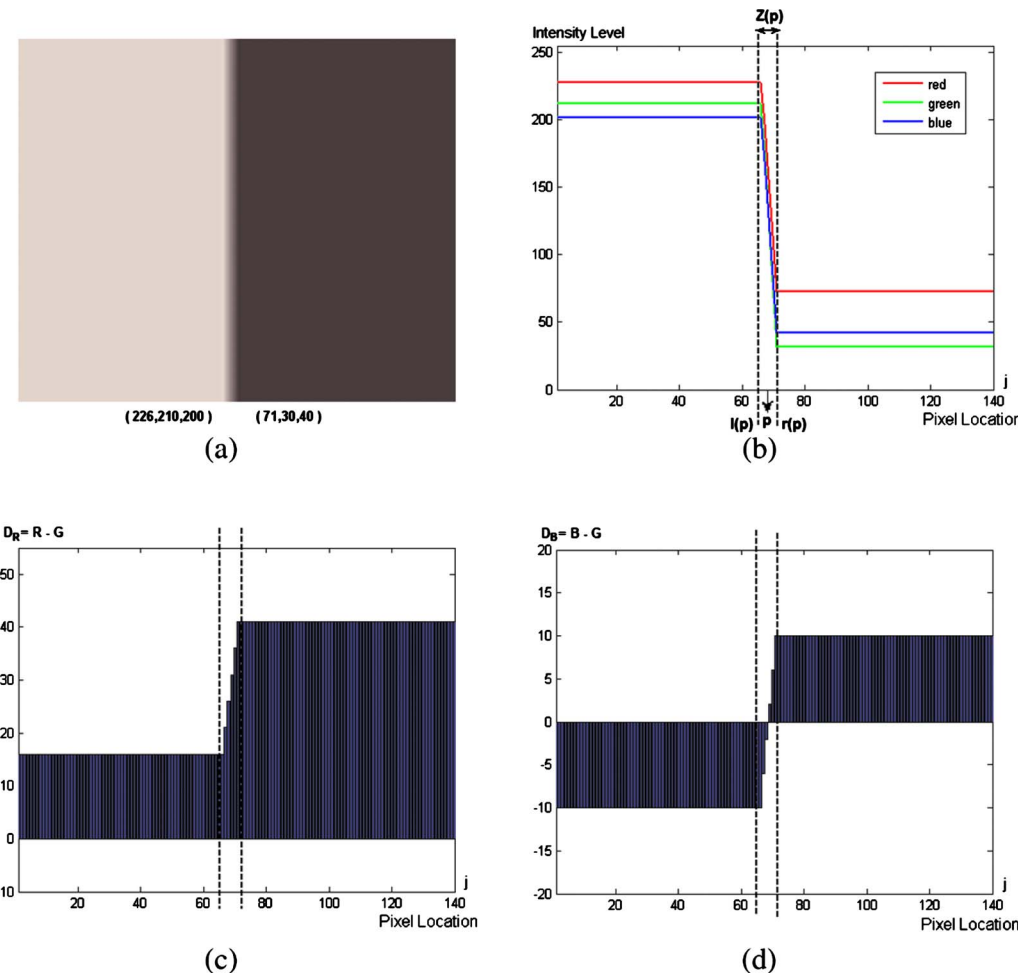


Fig. 2 Color behavior on a normal edge. (a) An edge without chromatic aberration. (b) RGB intensity along horizontal line of (a). (c) Color difference signal between the red and the green components. (d) Color difference signal between the blue and the green components. (Color online only.)

processing methods using the proposed range limitation condition are described. Experimental results are presented in Sec. 4, and last, Sec. 5 is the conclusion.

2 Color Behavior on Edges

Every edge has a transition region where color variation occurs. Suppose that p is a pixel location inside the transition area (see Fig. 2). The transition region can be defined as the area in which the RGB color state varies from (226, 210, 200) to (71, 30, 40). Starting from the left side, we can define the pixel location where color state starts to vary as $l(p)$ and the pixel location where color state stops varying as $r(p)$. Then, the transition region $Z(p)$ is derived as a set of pixels located between $l(p)$ and $r(p)$. Chromatic correlation²⁵ exists on normal edges that do not suffer chromatic aberration. The transition regions for each color component have the same width and position on normal edges [see Fig. 2(b)]. In this situation, there exists an interesting color behavior related to color difference signals. The color difference signals of each pixel are computed as the difference between the red (R) and the green (G) signals, and as the difference between the blue (B) and the green (G) signals in the RGB color space. Similar to the chroma com-

ponents usually expressed with color differences in YCbCr color spaces, the green signal is used as a reference signal for the difference calculation because it plays a dominant role on the luminance. The color difference signals have a certain property on normal edges. That is, each color difference signal in $Z(p)$ is higher than the minimum of the values at either $l(p)$ or $r(p)$, and lower than the maximum of the values at either $l(p)$ or $r(p)$. We represent this property as

$$\begin{aligned} \min\{D_R[l(p)], D_R[r(p)]\} &\leq D_R(j) \\ &\leq \max\{D_R[l(p)], D_R[r(p)]\}, \\ \min\{D_B[l(p)], D_B[r(p)]\} &\leq D_B(j) \\ &\leq \max\{D_B[l(p)], D_B[r(p)]\}, \end{aligned} \quad (1)$$

where $D_R(\cdot) = R(\cdot) - G(\cdot)$, $D_B(\cdot) = B(\cdot) - G(\cdot)$, and j is the pixel location in the transition region—that is, $j \in Z(p)$. This means that the color difference signals in the transition region are limited between the values of the corresponding boundary pixels. We call this the color difference property for edges.

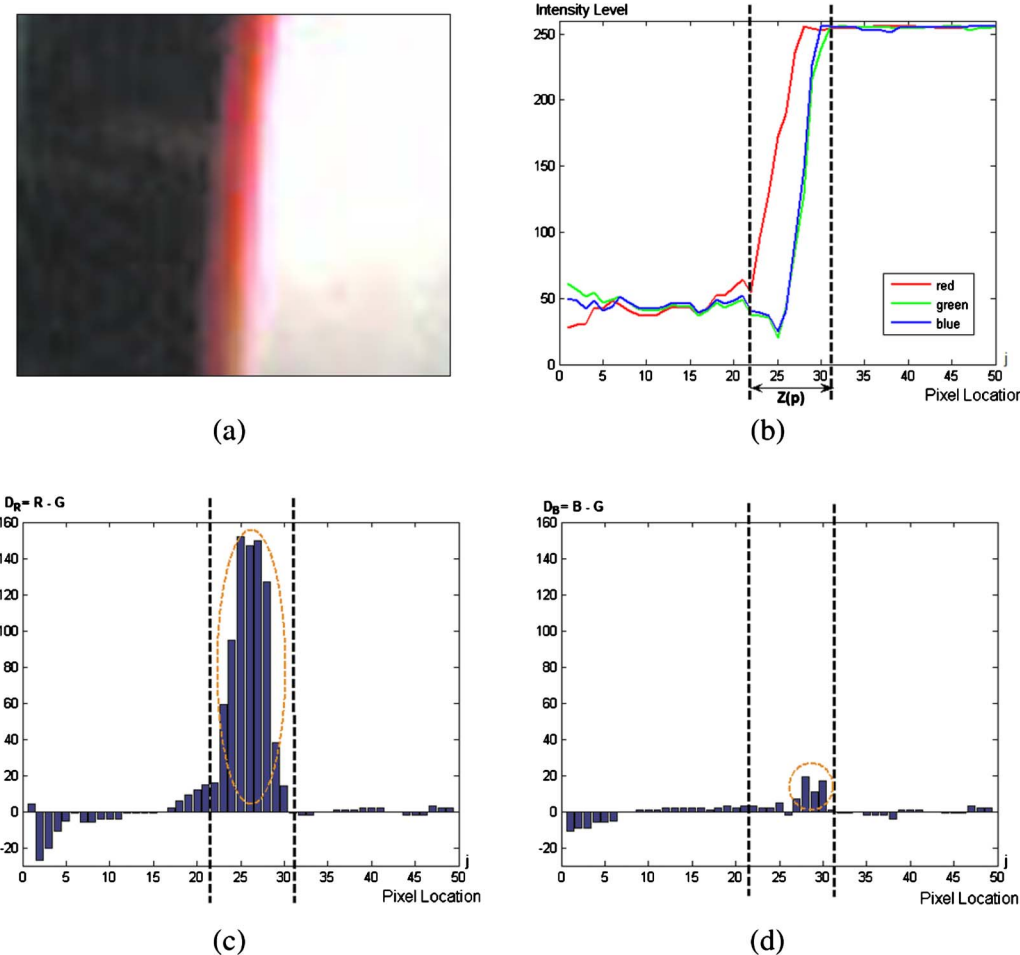


Fig. 3 Color behavior on a degraded edge (due to the lateral aberration): pixels violating the proposed condition are marked with orange dotted circles in (c) and (d). (a) A degraded edge with approximately 7-pixel-width red color fringes. (b) RGB intensity along horizontal line of (a). (c) Color difference signal between the red and the green components. (d) Color difference signal between the blue and the green components. (Color online only.)

In contrast, the edges with chromatic aberration violate the preceding property. Given an image with strong red color fringes caused by chromatic aberration [see Fig. 3(a)], plots of the RGB intensity along the horizontal direction reveal a geometrical shift to the left in the red signal due to lateral aberration. This aberration breaks the chromatic correlation, which means that the varying locations between each color component differ. $Z(p)$, the transition region between the two stable color values, can be defined as the set of pixels where at least one color component varies, or as the union of the different color components' transition regions. The color difference signals in Figs. 3(c) and 3(d) demonstrate that some pixels inside the transition region violate the proposed color difference property for edges, and we can specify that these pixels exhibit unpleasing color fringes around the edge. Figure 4 shows the occurrence of the longitudinal aberration edge. As shown in Figs. 4(c) and 4(d), there also exist some pixels that violate the proposed property so that the maximum values of the color difference signals are found inside the transition region. A strong blue color fringe is emphasized on the image edge because the color differences between the blue and the

green intensities are much larger than the differences between the red and the green intensities. Based on these observations, we will use this color difference property for edges to detect the aberration areas.

3 Removing Chromatic Aberration

To apply the color difference property for edges, we first need to identify the transition regions from a given image. The color components of an input image are denoted by $R(i, j)$, $G(i, j)$, and $B(i, j)$, where i and j represent the pixel location in the row and the column, respectively. The variation of each color intensity is detected by a gradient operation that is based on the widely used Sobel operators.²⁶

Our algorithm separately processes data in the horizontal direction and the vertical direction. For simplicity, we describe it with the horizontal direction. In the horizontal processing, all 2-D signals can be considered as 1-D cases with a fixed integer i as follows:

$$R(i, j), G(i, j), B(i, j), E_C(i, j) \Rightarrow R(j), G(j), B(j), E_C(j), \quad (2)$$

where

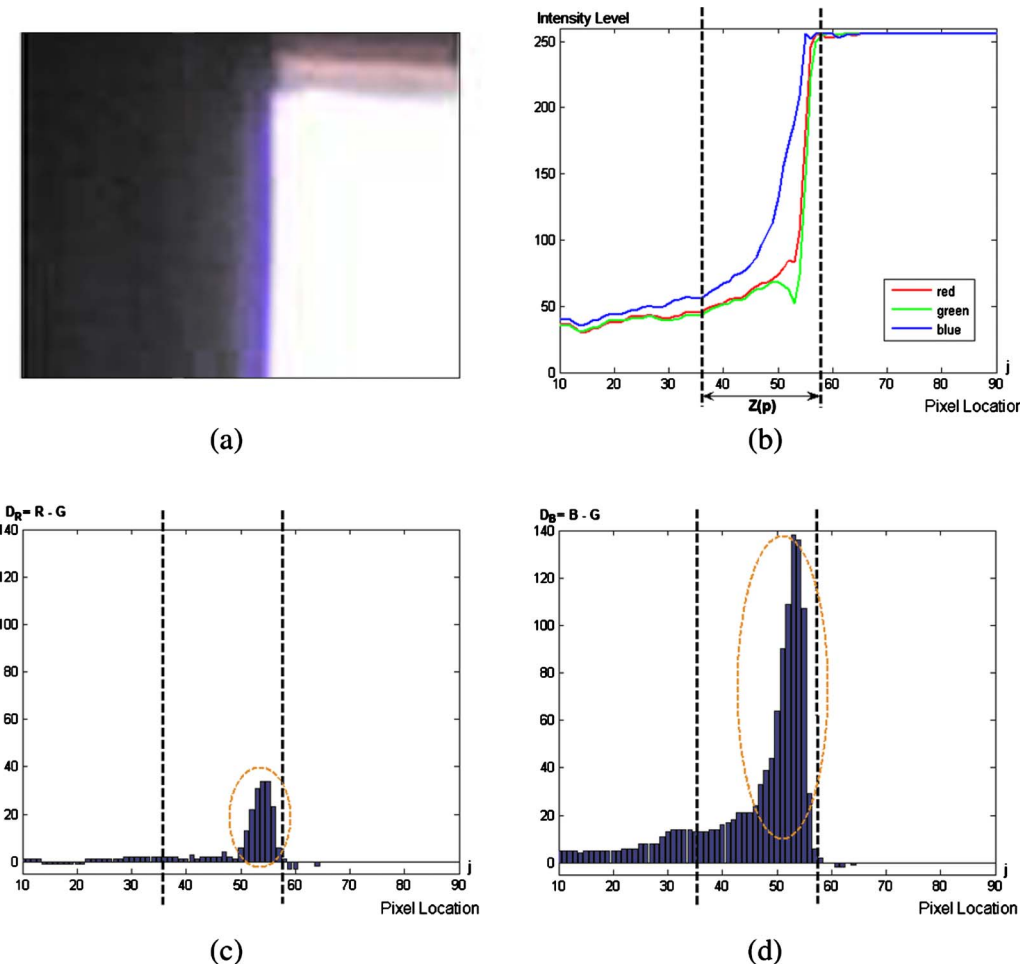


Fig. 4 Color behavior on a degraded edge (due to the longitudinal aberration): pixels violating the proposed condition are marked with orange dotted circles in (c) and (d). (a) A degraded edge with approximately 12-pixel-width blue color fringes. (b) RGB intensity along horizontal line of (a). (c) Color difference signal between the red and the green components. (d) Color difference signal between the blue and the green components. (Color online only.)

$$E_C(i,j) = C(i-1,j-1) + 2C(i,j-1) + C(i+1,j-1) - C(i-1,j+1) - 2C(i,j+1) - C(i+1,j+1), \quad (3)$$

which is the gradient value calculated with the vertical Sobel mask and $C \in \{R, G, B\}$. If the algorithm is applied for the other direction, the vertical operation, the horizontal Sobel mask must be used for calculating $E_C(i,j)$.

3.1 Determining Transition Regions

The transition region is the union of the pixels where at least one of the color values varies. A pixel will be identified as a part of a transition region when one of the gradient magnitudes is larger than or equal to a positive threshold T . In fact, because the green signal plays a dominant role on the luminance, the lens in most cameras is focused on the green. Considering that the green spectrum is located in the middle of the visible ray, focusing on the green signal is reasonable to avoid a biased chromatic aberration. Consequently, gradient values for the red and the blue includes all geometrically shifted and blurred information that is caused by chromatic aberration. In addition, most regions in an

image are flat with small color variation. Hence, instead of computing the three gradients for every pixel, we take only the green gradient to determine the initial point p and then search the whole transition region $Z(p)$ by calculating all three gradients adjacent to the initial point p .

The search procedure for the transition region is composed of three steps. Starting with $j=1$, the first step is to find the initial point p by increasing the pixel location j one by one until the green gradient magnitude becomes greater than or equal to T , as follows:

$$j \leftarrow j + 1 \quad \text{while } |E_G(j)| < T,$$

$$\text{set } p = j \quad \text{if } |E_G(j)| \geq T. \quad (4)$$

The pixel location p must be located in a transition area, so the search starts from this point for the transition region.

In the second step, starting from the initial point p , the left and the right transition width m and n , respectively, are calculated for the transition region $Z(p)$, as shown in Fig. 5. Initially, m and n are set to zero. The transition region with

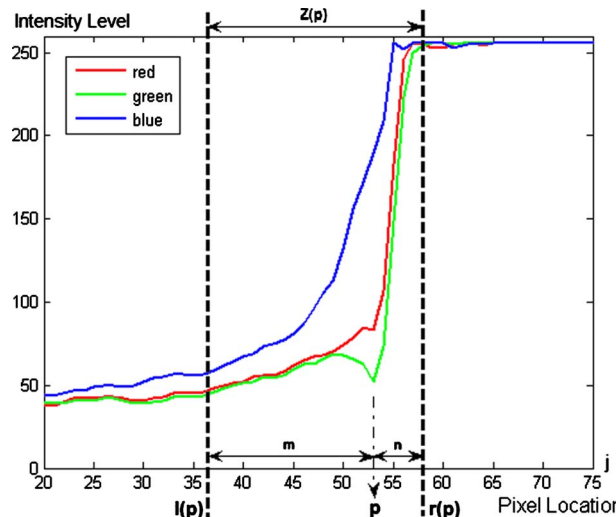


Fig. 5 Left transition width m and the right transition width n from the initial point p .

chromatic aberration has the same sign for R, G, and B gradient values, which means that the intensity level of each color component slants in the same direction. Thus, the sign of the gradient value of the green signal at the initial point p ,

$$s(p) = \text{sgn}[E_G(p)], \quad (5)$$

is computed first, and then we observe whether the adjacent pixels' gradient value has the same sign as $s(p)$. A pixel can be considered as a part of the transition region even if just one color component varies. The largest gradient value among R, G, and B at x that has a similar edge to G at a given initial point p is defined as follows:

$$H(x|p) = \max\{s(p)E_R(x), s(p)E_G(x), s(p)E_B(x)\}, \quad (6)$$

where x is the pixel located adjacent to the point p . A pixel at x is classified into the following three cases depending on the $H(x|p)$ value:

- Case 1, $H(x|p) < 0$: All three color values at x have the opposite gradient polarity to the green value at p .
- Case 2, $0 \leq H(x|p) < T$: At least one color signal at x has the same gradient polarity with the green signal at p , but the gradient magnitude is not large enough to justify as the presence of an edge.

- Case 3, $T \leq H(x|p)$: x can be considered as a part of the transition region because at least one color component has an edge similar to that of the green signal at p .

The transition widths m and n are increased as x moves to the left and the right side from the initial point p , respectively, as long as $H(x|p)$ satisfies the condition in case 3. The width increment will stop at the first left and right point, independently, where $H(x|p)$ becomes less than T . As a result, the left and the right boundary pixel locations, $l(p)$ and $r(p)$, are calculated as

$$l(p) = p - m, \quad (7)$$

and

$$r(p) = p + n, \quad (8)$$

and then the final transition region $Z(p)$ detected for the initial point p is defined as

$$Z(p) = \{j | l(p) < j < r(p)\}. \quad (9)$$

The search for the next transition region starts from $r(p)+1$ with checking the gradient value of the green signal, as in Eq. (4).

3.2 Detecting and Eliminating Chromatic Aberration

Chromatic aberration is detected independently in the red and the blue signals by searching for the pixels inside the transition region that violate the color difference property for edges. Because the color differences in these pixels are mainly responsible for undesirable color fringes, the elimination process corrects the color difference values of the detected pixels to remain inside the proper range. New color difference values are chosen between the two color difference values at $l(p)$ and $r(p)$. The pixels with color difference values larger than the maximum difference values at either $l(p)$ or $r(p)$ are replaced by the maximum difference values at either $l(p)$ or $r(p)$. On the other hand, the pixels where the color difference values are smaller than the minimum difference values at either $l(p)$ or $r(p)$ are replaced by the minimum difference values at either $l(p)$ or $r(p)$. After adjusting the color difference signals, the original green input signal is added to compute the corrected red and blue pixel values. Output RGB signals are expressed as

$$\hat{R}(j) = \begin{cases} \min\{D_R[l(p)], D_R[r(p)]\} + G(j), & \text{if } D_R(j) < \min\{D_R[l(p)], D_R[r(p)]\} \\ \max\{D_R[l(p)], D_R[r(p)]\} + G(j), & \text{if } D_R(j) > \max\{D_R[l(p)], D_R[r(p)]\}, \\ R(j), & \text{otherwise} \end{cases} \quad (10)$$

$$\hat{B}(j) = \begin{cases} \min\{D_B[l(p)], D_B[r(p)]\} + G(j), & \text{if } D_B(j) < \min\{D_B[l(p)], D_B[r(p)]\} \\ \max\{D_B[l(p)], D_B[r(p)]\} + G(j), & \text{if } D_B(j) > \max\{D_B[l(p)], D_B[r(p)]\}, \\ B(j), & \text{otherwise} \end{cases} \quad (11)$$

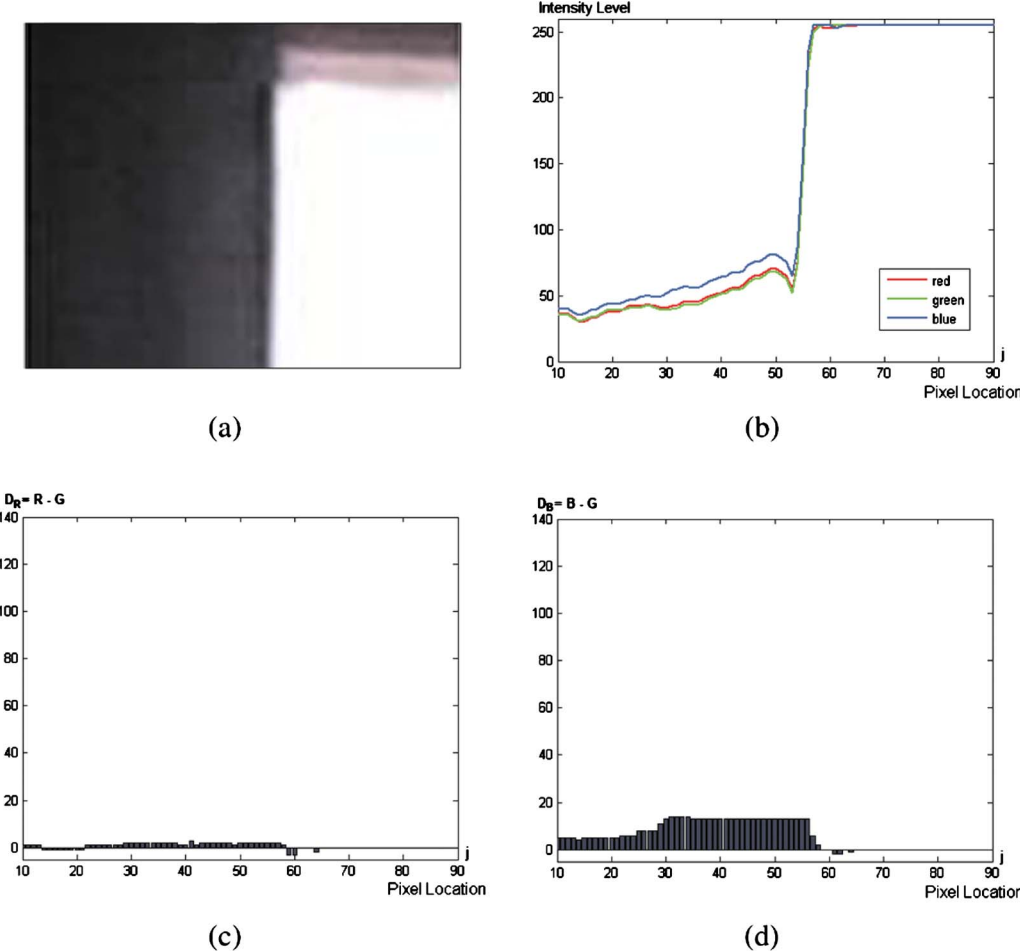


Fig. 6 Color difference compensation for eliminating chromatic aberration from the image in Fig. 4(a). (a) Corrected edge images. (b) RGB intensity along horizontal line of (a). (c) Corrected color difference between the red and the green components. (d) Corrected color difference between the blue and the green components. (Color online only)

$$\hat{G}(j) = G(j), \quad (12)$$

where $j \in Z(p)$.

This method is applied to the image in Fig. 4(a), as shown in Fig. 6. Unlike the original color difference values in Figs. 4(c) and 4(d), Figs. 6(c) and 6(d) show that the undesirable color difference values in the transition region are replaced with the maximum color difference values of the corresponding boundary pixels so that the difference values remain inside the proper range satisfying the color difference property for edges. The geometric shift and the color blur in the red and the blue signals has been corrected, resulting in a clean edge without color fringes [see Figs. 6(a) and 6(b)].

4 Experimental Results

To verify the efficacy of the proposed method, the algorithm has been applied to several images acquired from various digital cameras. All of the test images were digitized to 8 bits for each color. The maximum absolute value of the Sobel gradient, $|E_C(j)|$, for an 8-bit digitized image is 1024. If T in Eq. (4) is set to a high value, insufficient elimination occurs for the longitudinal aberration because

the pixels where intensity level varies with gentle slope, mostly due to longitudinal aberration, are excluded from being detected as a transition region. On the contrary, when T is set to a low value, the algorithm becomes sensitive to noise. It is empirically found that $T=30$ generates satisfactory results for most images.

Figure 7 shows the results for two degraded images with different color fringe widths. Both Figs. 7(a) and 7(d) have a size of 1536×2048 pixels, and a 160×160 pixel area is enlarged from each image for close observation [see Figs. 7(b) and 7(e)]. Figure 7(b) shows very thick blue fringes, approximately 15 pixels in width, around the wood railing. Figure 7(e) shows purple fringes of only 3 pixels in width along the borders of the roofs. It can be seen that the proposed algorithm corrects both the thick and the thin color fringes [Figs. 7(c) and 7(f)].

Experimental results for various types of aberrations are given in Fig. 8. Figure 8(a) is an image of size 1536×2048 pixels, where red fringes are present along the edges of the image. Figure 8(d) shows two enlarged parts of the images before and after the elimination process. The proposed method effectively eliminates the red color fringes of approximately 10-pixel width that mostly occur

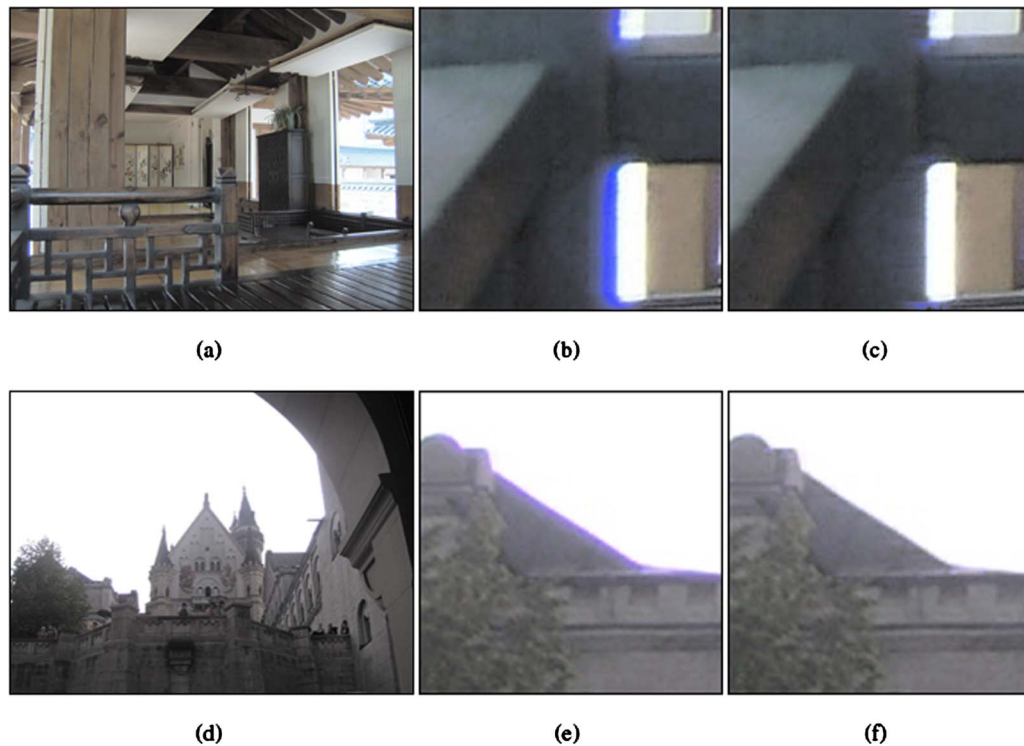


Fig. 7 Experimental results for the images with different color fringe widths. (a) House image. (b) Enlarged image of the bottom-left part of (a) (degraded PSNR=16.3292 dB, green PSNR=25.2519 dB). (c) Enlarged image of the aberration-eliminated result (corrected PSNR=25.0103 dB). (d) Cathedral image. (e) Enlarged image of the middle-left part of (d) (degraded PSNR=19.9807 dB, green PSNR=24.7617 dB). (f) Enlarged image of the aberration-eliminated result (corrected PSNR=24.4233 dB). (Color online only.)

due to lateral aberration. Figure 8(b) is an image of a car having size 1000×667 pixels. In Fig. 8(e), blue color fringes due to longitudinal aberration are also corrected properly. Last, Fig. 8(c) shows an image of size 960×1280 pixels with the most frequent purple fringes. Because the proposed method independently corrects both the red and the blue signal, the purple fringes are also eliminated successfully [see Fig. 8(f)].

Experiments were implemented in a MATLAB language program on an Intel Core2 Duo 3-GHz CPU PC with 2-GB RAM. The average operation CPU time for 20 color images of size 1536×2048 , including Figs. 7(a) and 7(d), was 1.413 s.

For a quantitative evaluation, we calculated a peak signal-to-noise ratio (PSNR) from a 16×16 region selected from one side of an edge where a color fringe appears. The PSNR is defined as

$$PSNR = 10 \log \left(\frac{255^2}{\sigma^2} \right) \quad (13)$$

where 255 represents the peak intensity value, and σ is a standard deviation. Since we use a color image, the standard deviation is calculated as a square root of the sum of each R, G, B variance divided by 3. If there were no color fringes, either side of an edge should be considered as a homogeneous area so that the standard deviation remains a small value. The results of the PSNR change are shown in Table 1. The corresponding green PSNR value, considered

as the reference signal, is illustrated also to help predict the amount of color fringes. For all the tested images, the PSNR measured in the color fringe region is smaller than the corresponding region's green PSNR. This is because that the red and the blue components keep varying even after the green component reaches a stable region due to chromatic aberration. However, color fringes are well eliminated after the correction process so that the PSNR value increases close to the corresponding green PSNR.

Last, to evaluate the performance of the proposed method, we compared the result with a reference image acquired using a 3MOS digital video camera, Panasonic HDC-TM200, in Fig. 9. We have photographed the same scene shown in Fig. 9(a) with two different cameras. Figure 9(b) shows an enlarged degraded image acquired with a CCD digital camera and the corresponding RGB intensity along the marked horizontal line. Inconsistencies exist between each color transition region in the edges so that color fringes are created along both edges. Using our method, the transition regions between each color are modified to be well matched so that the color fringes are well eliminated [see Fig. 9(c)]. Last, comparing the correction result with Fig. 9(d), the same region obtained with the 3MOS camera, we can observe that the proposed method is considerably more efficient.

5 Conclusion

This paper proposes a novel method for removing chromatic aberration using image processing from a single de-

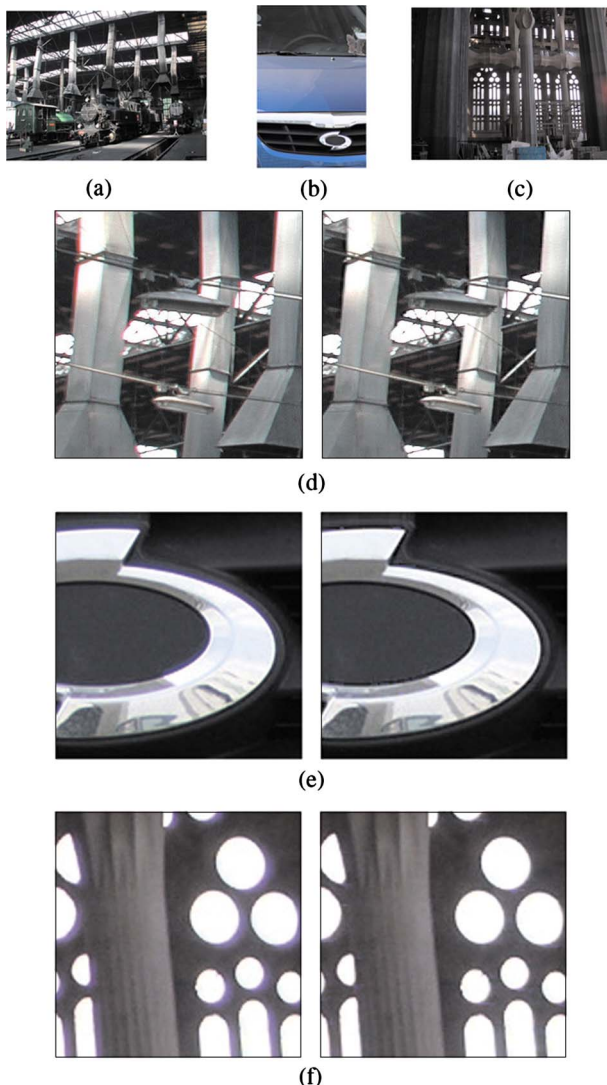


Fig. 8 Experimental results for the images degraded with various types of aberration. (a) Train image, (b) Car image, and (c) Church image. (d) Left: Enlarged image of the train image (degraded PSNR=16.3279 dB, green PSNR=22.3694 dB). Right: Enlarged image of the aberration-eliminated result (corrected PSNR=22.3713 dB; size: 300×300). (e) Left: Enlarged image of the car image (degraded PSNR=19.4502 dB, green PSNR=21.9965 dB). Right: Enlarged image of the aberration-eliminated result (corrected PSNR=22.0106 dB; size: 130×130). (f) Left: Enlarged image of the church image (degraded PSNR=18.4731 dB, green PSNR=22.4013 dB). Right: Enlarged image of the aberration-eliminated result (corrected PSNR=22.1513 dB; size: 130×130). (Color online only.)

graded image. We first analyze the color behavior of a normal image edge in terms of the color difference signals and show that the color fringes due to chromatic aberration can be detected using the color difference property for edges. We introduce a fast and simple algorithm that corrects the chromatic aberration by adjusting the color difference value between the red and the green signals and that between the blue and the green signals to remain inside the proper range.

Unlike previous algorithms, the proposed method detects and eliminates the color fringes directly from an input

Table 1 PSNR comparison of color fringe regions before and after the correction process.

	Green PSNR	Degraded PSNR	Corrected PSNR
House image	25.2519 dB	16.3292 dB	25.0103 dB
Cathedral image	24.7617 dB	19.9807 dB	24.4233 dB
Train image	22.3694 dB	16.3279 dB	22.3713 dB
Car image	21.9965 dB	19.4502 dB	22.0106 dB
Church image	22.4013 dB	18.4731 dB	22.1513 dB

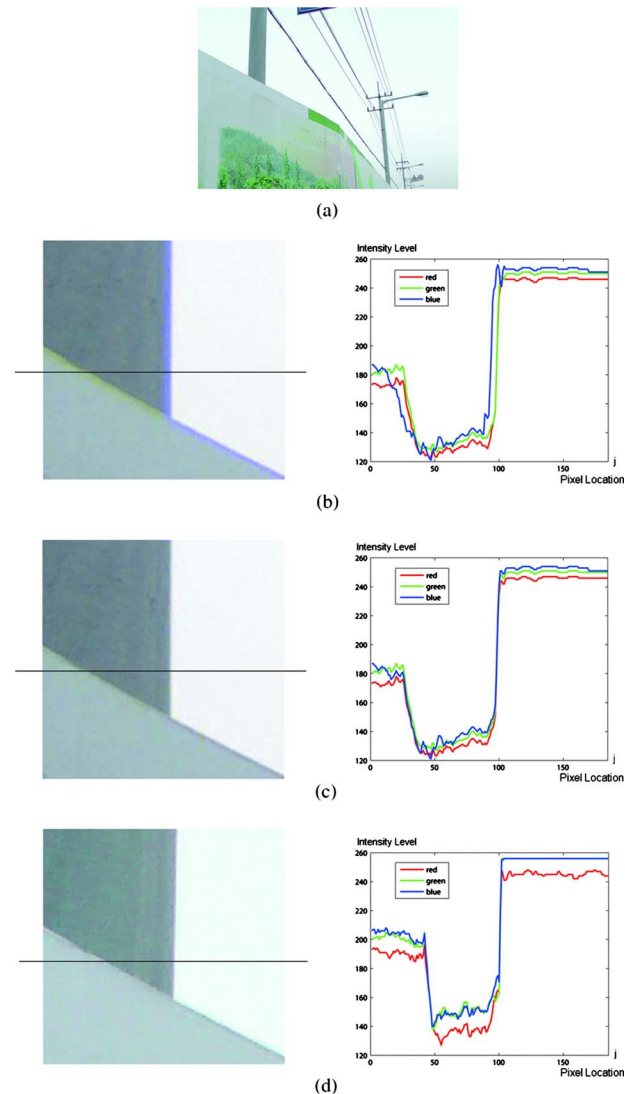


Fig. 9 Performance comparison. (a) Photographed scene. (b) Left: Enlarged degraded image photographed with an one-CCD camera (size: 185×185). Right: RGB intensity along the marked horizontal line. (c) Left: Enlarged image of the aberration-eliminated results (size: 185×185). Right: RGB intensity along the marked horizontal line. (d) Left: Enlarged image photographed with the 3MOS camera (size: 185×185). Right: RGB intensity along the marked horizontal line.

image. Hence, the method is free from the accuracy of the aberration kernel model and from the high computational complexity of the parameter estimation process. The algorithm significantly reduces both the lateral and the longitudinal aberrations without reference to the width of the color fringe or the type of aberration. Since the proposed algorithm requires no *a priori* knowledge, such as the precalibrated test pattern or a location of the aberration center, it can be easily applied to any image. The proposed method can be used in many real-time video camera applications with low computational complexity and simple 1-D separable structure.

Acknowledgments

This work was supported in part by the IT R&D program of MKE/MCST/IITA (2008-F-031-01, Development of Computational Photography Technologies for Image and Video Contents), in part by the Brain Korea (BK) 21 Program funded by MEST, and in part by the HY-SDR Research Center at Hanyang University under the ITRC Program of MKE, Korea.

References

1. J. R. Meyer-Arendt, *Introduction to Classical and Modern Optics*, 4th ed., Prentice Hall (1995).
2. C. C. Salma, *Manual of Photogrammetry*, 4th ed., American Society Photogrammetry, Falls Church, VA (1980).
3. P. B. Kruger, S. Mathews, K. R. Aggarwala, and N. Sanchez, "Chromatic aberration and ocular focus: Fincham revisited," *Vision Res.* **33**, 1397–1411 (1993).
4. V. Kaufmann and R. Lasdtter, "Elimination of color fringes in digital photographs caused by lateral chromatic aberration," in *Proc. XX Int. Symp. CIPA*, pp. 403–408 (2005).
5. T. Luhmann, H. Hastedt, and W. Tecklenburg, "Modeling of chromatic aberration for high precision photogrammetry," in *Commission V Symp. on Image Engineering and Vision Metrology, Proc. ISPRS*, **36**(5), 173–178 (2006).
6. I. Powell, "Lenses for correcting chromatic aberration of the eye," *Appl. Opt.* **20**(24), 4152–4155 (1981).
7. G. H. Smith, *Practical Computer-Aided Lens Design*, Willmann-Bell, Richmond, VA (1998).
8. N. R. Farrar, A. H. Smith, D. R. Busath, and D. Taitano, "In situ measurement of lens aberration," *Proc. SPIE* **4000**, 18–29 (2000).
9. M. S. Millan, J. Oton, and E. Perez-Cabre, "Chromatic compensation of programmable Fresnel lenses," *Opt. Express* **14**(13), 6226–6242 (2006).
10. M. S. Millan, J. Oton, and E. Perez-Cabre, "Dynamic compensation of chromatic aberration in a programmable diffractive lens," *Opt. Express* **14**(20), 9103–9112 (2006).
11. Y. C. Fang, T. K. Liu, J. Macdonald, J. H. Chou, B. W. Wu, H. L. Tsai, and E. H. Chang, "Optimizing chromatic aberration calibration using a novel genetic algorithm," *J. Mod. Opt.* **53**(10), 1411–1427 (2006).
12. R. Kingslake, *Lens Design Fundamentals*, Academic Press, New York (1978).
13. R. G. Willson and S. A. Shafer, "Active lens control for high precision computer imaging," in *IEEE Int. Conf. on Robotics and Automation*, Vol. 3, pp. 2263–2070 (1991).
14. R. G. Willson, "Modeling and calibration of automated zoom lenses," PhD Thesis, Carnegie Mellon University (1994).
15. T. E. Boult and G. Wolberg, "Correcting chromatic aberration using image warping," in *IEEE Conf. on Computer Vision and Pattern Recognition*, pp. 684–687 (1992).
16. M. Rebiai, S. Mansouri, F. Phinson, and B. B. Tichit, "Image distortion from zoom lenses: modeling and digital correction," in *Proc. Int. Broadcasting Convention*, pp. 438–441 (1992).
17. M. K. Johnson and H. Farid, "Exposing digital forgeries through chromatic aberration," in *Proc. ACM Multimedia and Security Work-*shop, pp. 48–55 (2006).
18. J. Mallon and P. F. Whelan, "Calibration and removal of lateral chromatic aberration in images," *Pattern Recogn. Lett.* **28**(1), 125–135 (2007).
19. R. G. Willson and S. A. Shafer, "What is the center of the image?" *J. Opt. Soc. Am. A* **11**(11), 2946–2955 (1994).
20. S. B. Kang, "Automatic removal of chromatic aberration from a single image," in *Proc. IEEE Conf. Computer Vision and Pattern Recognition*, pp. 1–8 (2007).
21. M. Kozubek and P. Matula, "An efficient algorithm for measurement and correction of chromatic aberration in fluorescence microscopy," *J. Microsc.* **200**(3), 206–217 (2000).
22. E. M. M. Manders, "Chromatic shift in multicolor confocal microscopy," *J. Microsc.* **185**, 321–328 (1997).
23. K. Shi, P. Li, S. Yin, and Z. Liu, "Chromatic confocal microscopy using supercontinuum light," *Opt. Express* **12**, 2096–2101 (2004).
24. B. Freitag, S. Kujawa, P. Mul, J. Ringnalda, and P. Tiemeijer, "Breaking the spherical and chromatic aberration barrier in transmission electron microscopy," *Ultramicroscopy* **102**, 209–214 (2005).
25. M. Kobayashi, M. Noma, S. Hiratsuka, and S. Kamata, "Lossless compression for RGB color still images," in *Int. Conf. on Image Processing* Vol. 4, pp. 73–77 (1999).
26. R. C. Gonzalez and R. E. Woods, *Digital Image Processing*, 2nd ed., Prentice Hall (2002).



Soon-Wook Chung received his BS degree in electronics engineering from Sungkyunkwan University in 2002. Since 2003, he has been a research assistant at the Department of Electronic and Electrical Engineering, Pohang University of Science and Technology (POSTECH), where he is currently working toward his PhD degree. His research interests include digital image processing—in particular, computational photography, signal processing for digital television, and image enhancement.



Byoung-Kwang Kim received his BS degree in electronics engineering from Pohang University of Science and Technology (POSTECH) in 2008. Since 2008, he has been a research assistant at the Department of Electronic and Electrical Engineering, POSTECH, where he is currently working toward his PhD degree. His research interests include digital image processing—in particular, computational photography and signal processing for digital television.



Woo-Jin Song received his BS and MS degrees in electronics engineering from Seoul National University in 1979 and 1981, respectively, and his PhD degree in electrical engineering from Rensselaer Polytechnic Institute in 1986. During 1981 to 1982, he worked at the Electronics and Telecommunication Research Institute (ETRI), Korea. In 1986, he was employed by Polaroid Corporation as a senior engineer, working on digital image processing. In 1989, he joined the faculty at Pohang University of Science and Technology (POSTECH), Korea, where he is a professor of electronic and electrical engineering. His current research interests are in the area of digital signal processing—in particular, radar signal processing, signal processing for digital television and multimedia products, and adaptive signal processing.